Journal of Organometallic Chemistry 853 (2017) 149–158

Contents lists available at ScienceDirect

Journal of Organometallic Chemistry

journal homepage: www.elsevier.com/locate/jorganchem

Anionic polymerization of multi-vinylferrocenes

Khaled Al Khalyfeh [a, b], Jonas F. Nawroth [c], Martin Uhlemann [d], Ulrich Stoeck [d], Lars Giebeler [d], Rainer Jordan [c], Alexander Hildebrandt [a, *]

[a] Technische Universität Chemnitz, Faculty of Natural Sciences, Institute of Chemistry, Inorganic Chemistry, D-09107 Chemnitz, Germany
[b] Al-Hussein Bin Talal University, Faculty of Natural Sciences, Department of Chemistry, P.O. Box 20, Ma'an, Jordan
[c] Technische Universität Dresden, School of Science, Chair of Macromolecular Chemistry, Mommsenstr. 4, D-01069 Dresden, Germany
[d] Leibniz Institute for Solid State and Materials Research (IFW) Dresden e.V., Institute for Complex Materials, Helmholtzstr. 20, D-01069 Dresden, Germany

ARTICLE INFO

Article history:
Received 21 August 2017
Received in revised form
9 October 2017
Accepted 12 October 2017
Available online 18 October 2017

Keywords:
Anionic polymerization
Polyvinylferrocenes
Cross-linked
Electrochemistry
Li-ion battery
Rechargeable battery

ABSTRACT

Protocols for anionic polymerization of vinylferrocenes in bulk (**b**) and solution (**s**) are reported. Polymerization of vinylferrocenes bearing one or multiple (2–4) vinyl groups yielded linear polyvinylferrocene **PVF-1**(**b, s**) or cross-linked polyvinylferrocenes **PVF-2** – **PVF-4**(**b, s**), respectively. Furthermore, copolymerization of mono-with multifunctional vinylferrocenes produced cross-linked copolymers **PVF-5** – **PVF-7**(**b, s**). For anionic polymerization in bulk, a high monomer conversion and a relatively high dispersity was observed. A reversible redox behavior of the ferrocenyl group with cycle stability up to 100 cycles was found for **PVF-**(**1s** – **7s**). Li-ion battery cell tests demonstrated the applicability of the polyvinylferrocenes **PVF-1b** and **PVF-**(**5b** – **7b**) as electrode materials.

1. Introduction

Ferrocene and its derivatives have been in the focus of research for several decades due to their intriguing magnetic, electrical and electrochemical properties [1–4]. Today, 65 years after the discovery of ferrocene [4–6], ferrocenyl functionalities have been incorporated into different polymer backbones [7–12] introducing properties, such as, a pronounced electron donating ability, fast electrochemical response, high thermal stability and redox reversibility [11–17]. These properties allow for such polymers to be used in a variety of applications including electrochemical sensors [18–23], biosensors [24], thin film transistors [25], light emitting diodes [26], molecular magnets [27,28], as well as semiconductors [29–32], conductors [12,33,34] and charge storage materials [14,33,35–38].

The first well-characterized ferrocene-containing polymer was prepared in 1955 *via* free radical and cationic polymerization of vinylferrocene [7]. In 1992 the feasibility of the anionic polymerization of vinylferrocene has been shown [39,40]. Subsequent improvements of the polymerization reaction by systematic variations of the reaction conditions have been reported [20]. [41–47].

Especially due to their electrochemical properties, polyferrocene materials are sought after in the development of cathode materials within Li-ion batteries technology [48,49]. One challenge arises from the easy solubility in the electrolyte which in general appears when these polymers are used as cathode material in battery applications. This chemical nature often leads to a degradation of the cathode after several charge/discharge cycles [37]. [50,51] Therefore, we aim to introduce cross-linking units to decrease the solubility, while still maintaining a high "ferrocene" content of the polymer. Herein, we present the anionic polymerization in bulk and solution of different vinylferrocenes for the synthesis of linear and cross-linked PVFs. Furthermore, their electrochemical behavior and the possible use for Li-ion batteries are reported.

2. Materials and methods

2.1. General data

All lithiation reactions were carried out under an argon (5.0) atmosphere using standard Schlenk techniques. Tetrahydrofuran

* Corresponding author.
E-mail address: alexander.hildebrandt@chemie.tu-chemnitz.de (A. Hildebrandt).

https://doi.org/10.1016/j.jorganchem.2017.10.009
0022-328X/

(THF) was purified by distillation from sodium/benzophenone and toluene was obtained from a MBraun (MB-SPS 800) solvent purification system (double column solvent filtration, working pressure 0.5 bar). For electrochemistry HPLC grade dichloromethane (DCM) was purified by distillation from calcium hydride.

2.2. Instruments

A Bruker Avance III 500 spectrometer operating in the Fourier transform mode at 298 K was used to record the NMR spectra (^{1}H NMR (500.3 MHz) and ^{13}C{^{1}H} NMR (125.8 MHz)), whereas the undeuterated residues (chloroform; ^{1}H at 7.26 ppm) in deuterated solvent (chloroform-d_1; ^{13}C{^{1}H} at 77.00 ppm) served as internal standard (chemical shifts in δ, parts per million). A Bruker Avance 400 spectrometer equipped with double-tuned probes capable of MAS (magic angle spinning) was used to record the solid state NMR spectra (^{1}H-MAS NMR (400.1 MHz) and ^{13}C{^{1}H} CP-MAS NMR (100.6 MHz)). Spinning 3.2 mm zirconium oxide rotors are used for sample packing at 15 kHz. ^{1}H-MAS NMR was obtained with single puls excitation (90° puls, puls length 2.4 μs) and a recycle delay of 6 s. Cross polarization (CP) technique with contact time of 3 ms is used to enhance sensitivity for acquiring the spectra. The ^{13}C-{^{1}H}-CP-MAS NMR is collected with ^{1}H decoupling using a TPPM (two puls phase modulation) puls sequence with 6 s recycle delaying. The spectras are referenced to tetramethyl silane (TMS) using TTSS (tetrakis(trimethylsilyl)silane) as an internal secondary standard (3.55 ppm for ^{13}C, 0.27 ppm for ^{1}H). A FT-Nicolet IR 200 spectrometer was used to record the infrared spectra. Analytical pure samples were used to determine the melting points with a Gallenkamp MFB 595 010 M melting point apparatus; elemental analyses were performed using a Thermo FlashEA 1112 Series instrument; UV/Vis-NIR spectra were recorded between 280 and 3000 nm using a Carl Zeiss MCS 400 spectrometer utilizing CLD 300 (210–600 nm) and CLX 11 lamps (300–1010 nm); MALDI-ToF-MS was performed on a Biflex IV from Bruker Daltonics. Due to low solubility of the analyte, the samples were mixed in solid state with dithranol in a ratio of 3:1 (w/w), respectively. The mixture was pestelled and homogenized. Following this, a small amount (tip of a spatula) was placed on the target and 1 μL of $CHCl_3$ was added to fix the sample. The system was calibrated against the peptide calibration standard II (Bruker) at sample conditions.

2.3. Electrochemistry

In solution: Electrochemical measurements were performed with 0.5 mmol·L^{-1} solutions of the analytes **PVF-(1s – 7s)** and 1.0 mmol·L^{-1} [N^{n}Bu$_4$][B(C$_6$F$_5$)$_4$] as supporting electrolyte in anhydrous DCM at 25 °C. The instrumentation consists of a Radiometer Volta-lab PGZ 100 electrochemical workstation interfaced with a personal computer. The measurement cell contains three electrodes, a Pt auxiliary electrode, a glassy carbon working electrode, and an Ag/Ag^{+} (0.01 mol·L^{-1} $AgNO_3$) reference electrode [52–58]. The working electrode was pretreated by polishing on a Buehler microcloth subsequently with 1 μm and 1/4 μm diamond paste. Under these conditions all experiments showed that all oxidation and reduction processes were reproducible within 5 mV. All experimental potentials were internally referenced against an Ag/Ag^{+} reference electrode whereas all presented results are referenced against ferrocene (as internal standard) as recommended by IUPAC [59]. The experimentally measured potential was converted into *E vs.* FcH/FcH^{+} (according our conditions the Fc*/Fc^{*+} couple was at −614 mV *vs.* FcH/FcH^{+}, ΔE_p = 60 mV, while the FcH/FcH^{+} couple itself was at 220 mV *vs.* Ag/Ag^{+}, ΔE_p = 61 mV) [60–62].

2.4. Solid state electrochemistry

For electrode preparation a slurry containing 30 wt% polyvinylferrocene, 30 wt% polyvinylidene difluoride (PVDF, Solvay) and 40 wt% C65 carbon (Timcal) in 1.5 mL *N*-methyl-pyrrolidone (VWR) was drop-coated onto 12 mm aluminum discs. Electrodes were dried in air for 2 days at 80 °C and at 100 °C under vacuum for 12 h prior to cell assembly.

Electrodes were assembled in Swagelok test cells using a Whatman glass fiber separator (13 mm diameter) and 200 μl of electrolyte and a lithium foil counter electrode (12 mm diameter, 250 μm thickness, Chempur). The electrolytes consisted of 1.5 M $LiPF_6$ (Sigma Aldrich) in 30 vol% ethylene carbonate (EC, Merck) and 70 vol% diethyl carbonate (DEC, Merck).

Test cells were cycled at 25 °C in a climate chamber using a VMP 3 potentiostat (Biologic). Cyclic voltammetry measurements were conducted in the potential range of 2.5 and 4.0 V *vs.* Li/Li^{+} with a scanning rate of 0.1 mV s^{-1}. Galvanostatic cycling experiments with potential limitation were conducted using a lower cutoff voltage of 2.5 V and a higher cutoff voltage of 4.0 V *vs.* Li/Li^{+} with a current rate of 10 mA·g$^{-1}{}_{PVF}$.

2.5. Spectroelectrochemistry

Spectroelectrochemical UV/Vis-NIR measurements of 0.25 mmol L^{-1} solution of (**PVF-1s** – **PVF-7s**) in anhydrous DCM containing 1 mmol L^{-1} of [N^{n}Bu$_4$][B(C$_6$F$_5$)$_4$] as supporting electrolyte were performed in an OTTLE (optically transparent thin-layer electrochemical) [63] cell with a Varian Cary 5000 spectrophotometer at 25 °C. A stepwise increasing within heights of 100, 50 or 25 mV have been used for the applied potentials among the spectroscopic measurements. To prove the reversibility of the oxidations, additional spectra were recorded after the potential was reduced to -500 mV for 15 min at the end of the measurements.

2.6. Reagents

All starting materials were obtained from commercial suppliers and used without further purification. Vinylferrocene **1** [41], 1,2-divinylferrocene **2** [64], 1,1′,2-trivinylferrocene **3** and 1,1′,2,2′-tetravinylferrocene **4** [52] were synthesized according to published procedures.

2.7. Synthesis

2.7.1. General procedure for bulk polymerization

Vinylferrocene **1**, 1,2-divinylferrocene **2**, 1,1′,2-trivinylferrocene **3** or 1,1′,2,2′-tetravinylferrocene **4** were stirred at 70 °C for 1 min and ^{n}BuLi (0.01 eq) was added in one portion. After stirring for 2 min, the mixture start to solidify and anhydrous toluene (0.15 mL per 1 mmol of monomer) was added and stirring was continued for 1 h. After the addition of methanol (1.0 eq) at 25 °C and stirring for 15 min, the mixture was concentrated to 2 mL in vacuum. The reaction mixture was dropped in methanol (150 mL per 1 g of monomer), the product was then filtered off, washed with 20 mL of hexane and diethyl ether and dried in oil pump vacuum for 24 h.

*2.7.1.1. Synthesis of poly(vinylferrocene) (**PVF-1b**).* Vinylferrocene **1** (1.0 eq, 1.50 g, 7.1 mmol), ^{n}BuLi (0.01 eq, 2.5 M in hexane, 28.3 mmL, 70.7 μmol). Product: 1.42 g, 94.7% as yellow powder; MALDI-TOF (g·mol^{-1}): 2638 (D = 1.46); elemental analysis calculated for ((C$_{12}$H$_{12}$Fe)$_n$·(C$_4$H$_9$)$_{0.01n}$) (212.71 g mol^{-1})$_n$: C, 67.98; H, 5.72. Found: C, 67.46; H, 5.98; ^{1}H NMR ($CDCl_3$, *δ/ppm*): 4.81–3.25 (C$_{10}$H$_9$), 2.71–0.43 (C$_2$H$_3$); ^{13}C NMR ($CDCl_3$, *δ/ppm*): 68.6 (C$_5$H$_4$), 67.1 (C$_5$H$_5$), 32.1 (C$_2$H$_3$), 27.1 (C$_2$H$_3$), 22.9 (C$_2$H$_3$), 14.3

(C_2H_3),; IR (KBr, cm^{-1}): 3090 (m), 2925 (m), 2852 (m), 1622 (m), 1461 (m), 1411 (m), 1339 (m), 999 (s), 812 (s).

*2.7.1.2. Synthesis of poly(-1,2-divinylferrocene) (**PVF-2b**).* 1,2-divinylferrocene **2** (1.0 eq, 1.50 g, 6.3 mmol), ^{n}BuLi (0.01 eq, 2.5 M in hexane, 25.2 mmL, 63.0 μmol). Product: 1.42 g, 93.9% as dark brown powder; MALDI-TOF ($g \cdot mol^{-1}$): 1757 (D = 1.2); elemental analysis calculated for $((C_{14}H_{14}Fe)_n \cdot (C_4H_9)_{0.01n})$ (238.75 g $mol^{-1})_n$: C, 70.62; H, 5.95. Found: C, 69.40; H, 6.62; ^{1}H-MAS NMR (TTSS, *δ/ppm*): 5.24 (C_2H_3), 4.07 ($C_{10}H_8$), 1.07 (C_2H_3); ^{13}C{^{1}H} CP-MAS NMR (TTSS, *δ/ppm*): 134.4 (C_2H_3), 112.4 (C_2H_3), 94.5 (^{t}C, C_5H_3), 82.7 (^{t}C-C_5H_3), 70.1 (C_5H_3), 66.7 (C_5H_5), 37.4 (C_2H_3), 32.9 (C_2H_3); IR (KBr, cm^{-1}): 3091 (m), 2924 (m), 2857 (m), 1623 (m), 1456 (m), 1412 (m), 1000 (s), 815 (s).

*2.7.1.3. Synthesis of poly(-1,1′,2-trivinylferrocene) (**PVF-3b**).* 1,1′,2-trivinylferrocene **3** (1.0 eq, 1.50 g, 5.7 mmol), ^{n}BuLi (0.01 eq, 2.5 M in hexane, 22.7 mmL, 56.8 μmol. Product: 1.45 g, 95.6% as black powder; MALDI-TOF ($g \cdot mol^{-1}$): 694 (D = 1.02); elemental analysis calculated for $((C_{16}H_{16}Fe)_n \cdot (C_4H_9)_{0.01n})$ (264.78 g $mol^{-1})_n$: C, 72.75; H, 6.13. Found: C, 73.05; H, 7.27; ^{1}H-MAS NMR (TTSS, *δ/ppm*): 7.07 (C_2H_3), 3.54 ($C_{10}H_7$), 1.31 (C_2H_3); ^{13}C{^{1}H} CP-MAS NMR (TTSS, *δ/ppm*): 133.8 (C_2H_3), 112.0 (C_2H_3), 90.6 (^{t}C-C_5H_3), 89.7 (^{t}C-C_5H_3), 83.8 (^{t}C-C_5H_4), 68.0 (C_5H_3, C_5H_4), 37.1 (C_2H_3), 33.8 (C_2H_3), 23.7 (C_2H_3), 14.7 (C_2H_3); IR (KBr, cm^{-1}): 3078 (m), 2914 (m), 2849 (m), 1625 (m), 1451 (m), 983 (s), 895 (m), 798 (s).

*2.7.1.4. Synthesis of poly(-1,1′,2,2′-tetravinylferrocene) (**PVF-4b**).* 1,1′,2,2′-tetravinylferrocene **4** (1.0 eq, 1.50 g, 5.2 mmol), ^{n}BuLi (0.01 eq, 2.5 M in hexane, 20.68 mmL, 51.7 μmol). Product: 1.46 g, 96.0% as black powder; MALDI-TOF ($g \cdot mol^{-1}$): 780 (D = 1.03); elemental analysis calculated for $((C_{18}H_{18}Fe)_n \cdot (C_4H_9)_{0.01n})$ (290.82 g $mol^{-1})_n$: C, 74.50; H, 6.27. Found: C, 74.69; H, 7.53; ^{1}H-MAS NMR (TTSS, *δ/ppm*): 7.10 (C_2H_3), 3.63 ($C_{10}H_6$), 1.01 (C_2H_3); ^{13}C{^{1}H} CP-MAS NMR (TTSS, *δ/ppm*): 134.3 (C_2H_3), 112.0 (C_2H_3), 89.4 (^{t}C-C_5H_3), 84.0 (^{t}C-C_5H_3), 67.8 (C_5H_3), 67.1 (C_5H_3), 41.4 (C_2H_3), 32.9 (C_2H_3), 23.1 (C_2H_3), 14.5 (C_2H_3); IR (KBr, cm^{-1}): 3078 (m), 2918 (m), 2853 (m), 1624 (m), 1448 (m), 980 (s), 892 (m), 797 (s).

*2.7.1.5. Synthesis of poly(vinylferrocene-co-1,2-divinylferrocene) (**PVF-5b**).* Vinylferrocene **1** (1.0 eq, 1.50 g, 7.1 mmol), 1,2-divinylferrocene **2** (0.1 eq, 0.17 g, 0.07 mmol), ^{n}BuLi (0.01 eq, 2.5 M in hexane, 31.1 mmL, 77.8 μmol). Product: 1.56 g, 93.4% as yellow powder; MALDI-TOF ($g \cdot mol^{-1}$): 1880 (D = 1.20); elemental analysis calculated for $((C_{12}H_{12}Fe)_n \cdot (C_{14}H_{14}Fe)_{0.1n})$ (235.87 g $mol^{-1})_n$: C, 68.2; H, 5.70. Found: C, 66.58; H, 5.86; ^{1}H NMR ($CDCl_3$, *δ/ppm*): 6.57–6.33 (C_2H_3), 5.58–4.89 (C_2H_3), 4.83–3.15 ($C_{10}H_9$, $C_{10}H_8$), 2.82–0.30 (C_2H_2); ^{13}C NMR ($CDCl_3$, *δ/ppm*): 134.8 (C_2H_3), 111.2 (C_2H_3), 69.4 (^{t}C-C_5H_4), 69.2 (^{t}C-C_5H_3), 68.8 (C_5H_4), 68.6 (C_5H_3), 67.1 (C_5H_5), 66.8 (C_5H_5), 35.3 (C_2H_3), 32.3 (C_2H_3), 22.9 (C_2H_3), 14.4 (C_2H_3); IR (KBr, cm^{-1}): 3089 (m), 2926 (m), 2855 (m), 1627 (m), 1459 (m), 1411 (m), 1340 (m), 999 (s), 814 (s).

*2.7.1.6. Synthesis of poly(vinylferrocene-co-1,1′,2-trivinylferrocene) (**PVF-6b**).* Vinylferrocene **1** (1.0 eq, 1.50 g, 7.1 mmol), 1,1′,2-trivinylferrocene **3** (0.1 eq, 0.19 g, 0.07 mmol), ^{n}BuLi (0.01 eq, 2.5 M in hexane, 31.1 mmL, 77.8 μmol). Product: 1.59 g, 94.1% as yellow powder; MALDI-TOF ($g \cdot mol^{-1}$): 1958 (D = 1.15); elemental analysis calculated for $((C_{12}H_{12}Fe)_n \cdot (C_{16}H_{16}Fe)_{0.1n})$ (238.48 g $mol^{-1})_n$: C, 68.5; H, 5.80. Found: C, 68.30; H, 6.20; ^{1}H-MAS NMR (TTSS, *δ/ppm*): 7.07 (C_2H_3), 3.54 ($C_{10}H_9$, $C_{10}H_6$), 1.31 (C_2H_3); ^{13}C{^{1}H} CP-MAS NMR (TTSS, *δ/ppm*): 133.7 (C_2H_3), 112.0 (C_2H_3), 90.6 (^{t}C-C_5H_4), 89.7 (^{t}C-C_5H_3, ^{t}C-C_5H_4), 83.8 (C_5H_4, C_5H_3), 68.0 (C_5H_5), 37.1 (C_2H_3), 33.8 (C_2H_3), 23.1 (C_2H_3), 14.5 (C_2H_3); IR (KBr, cm^{-1}): 3093 (m), 2921 (m), 2854 (m), 1632 (m), 1457 (m), 1411 (m), 1339 (m), 1000 (s), 813 (s), 751 (s).

*2.7.1.7. Synthesis of poly(vinylferrocene-co-1,1′,2,2′-tetravinylferrocene) (**PVF-7b**).* Vinylferrocene **1** (1.0 eq, 1.50 g, 7.1 mmol), 1,1′,2,2′-tetravinylferrocene **4** (0.1 eq, 0.21 g, 0.07 mmol), ^{n}BuLi (0.01 eq, 2.5 M in hexane, 31.1 mmL, 77.8 μmol. Product: 1.60 g, 93.6% as brownish-yellow powder; MALDI-TOF ($g \cdot mol^{-1}$): 1992 (D = 1.19); elemental analysis calculated for $((C_{12}H_{12}Fe)_n \cdot (C_{18}H_{18}Fe)_{0.1n})$ (241.09 g $mol^{-1})_n$: C, 68.7; H, 5.80. Found: C, 67.59; H, 6.25; ^{1}H-MAS NMR (TTSS, *δ/ppm*): 7.10 (C_2H_3), 4.13 ($C_{10}H_9$, $C_{10}H_6$), 1.01 (C_2H_3); ^{13}C{^{1}H} CP-MAS NMR (TTSS, *δ/ppm*): 134.3 (C_2H_3), 112.0 (C_2H_3), 89.4 (^{t}C-C_5H_4), 84.0 (^{t}C-C_5H_3, ^{t}C-C_5H_4), 67.8 (C_5H_4, C_5H_3), 67.1.0 (C_5H_5), 41.4 (C_2H_3), 32.9 (C_2H_3), 23.1 (C_2H_3), 14.5 (C_2H_3); IR (KBr, cm^{-1}): 3092 (m), 2922 (m), 2855 (m), 1620 (m), 1458 (m), 1411 (m), 1338 (m), 1000 (s), 814 (s).

2.7.2. General procedure for polymerization in solution

Vinylferrocene **1**, 1,2-divinylferrocene **2**, 1,1′,2-trivinylferrocene **3** or 1,1′,2,2′-tetravinylferrocene **4** were dissolved in anhydrous tetrahydrofuran (15 mL/1 mmol) and ^{n}BuLi (0.01 eq/vinyl group) was added in one portion at 25 °C and was stirred for 2 h. After addition of methanol (1.0 eq) and stirring for 15 min. The mixture was concentrated to 2 mL in vacuum. The reaction mixture was dropped in methanol (150 mL per 1 g of monomer), the product was then filtered off, washed with 20 mL of hexane and diethyl ether and dried in oil pump vacuum for 24 h.

*2.7.2.1. Synthesis of poly(vinylferrocene) (**PVF-1s**).* Vinylferrocene **1** (1.0 eq, 1.50 g, 7.1 mmol), ^{n}BuLi (0.01 eq, 2.5 M in hexane, 28.3 mmL, 70.7 μmol). Product: 1.23 g, 82.0% as yellow powder; MALDI-TOF ($g \cdot mol^{-1}$): 1896 (D = 1.65); elemental analysis calculated for $(C_{12}H_{12}Fe)_n$ (212.07 g $mol^{-1})_n$: C, 67.96; H, 5.70. Found: C, 67.46; H, 5.98; ^{1}H NMR ($CDCl_3$, *δ/ppm*): 4.54–3.49 ($C_{10}H_9$), 2.86–0.70 (C_2H_3); ^{13}C NMR ($CDCl_3$, *δ/ppm*): 68.6 (C_5H_4), 67.1 (C_5H_5), 32.3 (C_2H_3), 27.1 (C_2H_3), 22.8 (C_2H_3), 14.3 (C_2H_3); IR (KBr, cm^{-1}): 3087 (m), 2928 (m), 2847 (m), 1626 (m), 1458 (m), 1410 (m), 1336 (m), 1000 (s), 813 (s).

*2.7.2.2. Synthesis of poly(-1,2-divinylferrocene) (**PVF-2s**).* 1,2-divinylferrocene **2** (1.0 eq, 1.50 g, 6.3 mmol), ^{n}BuLi (0.01 eq, 2.5 M in hexane, 25.2 mmL, 63.0 μmol. Product: 1.22 g, 80.7% as dark brown powder; MALDI-TOF ($g \cdot mol^{-1}$): 2306 (D = 1.18); elemental analysis calculated for $((C_{14}H_{14}Fe)_n \cdot (C_4H_9)_{0.01n})$ (238.75 g $mol^{-1})_n$: C, 70.62; H, 5.95. Found: C, 69.41; H, 6.65; ^{1}H NMR ($CDCl_3$, *δ/ppm*): 6.50–6.37 (C_2H_3), 5.41–5.00 (C_2H_3), 4.57–3.55 ($C_{10}H_9$), 3.04–0.67 (C_2H_2); ^{13}C NMR ($CDCl_3$, *δ/ppm*): 133.0 (C_2H_3), 112.6 (C_2H_3), 70.5 (^{t}C-C_5H_3), 70.2–65.5 (C_5H_3), 69.4–68.7 (C_5H_3), 66.3 (C_5H_3), 65.8–65.3 (C_5H_5), 29.8 (C_2H_3), 22.8 (C_2H_3), 14.4 (C_2H_3), 14.3 (C_2H_3); IR (KBr, cm^{-1}): 3091 (m), 2922 (m), 2851 (m), 1625 (m), 1456 (m), 1409 (m), 999 (s), 814 (s).

*2.7.2.3. Synthesis of poly(-1,1′,2-trivinylferrocene) (**PVF-3s**).* 1,1′,2-trivinylferrocene **3** (1.0 eq, 1.50 g, 5.7 mmol), ^{n}BuLi (0.01 eq, 2.5 M in hexane, 22.7 mmL, 56.8 μmol). Product: 1.24 g, 81.7% as black powder; MALDI-TOF ($g \cdot mol^{-1}$): 957 (D = 1.06); elemental analysis calculated for $((C_{16}H_{16}Fe)_n \cdot (C_4H_9)_{0.01n})$ (264.78 g $mol^{-1})_n$: C, 72.75; H, 6.13. Found: C, 73.18; H, 7.28; ^{1}H NMR ($CDCl_3$, *δ/ppm*): 6.54–6.37 (C_2H_3), 5.41–4.97 (C_2H_3), 4.59–3.41 ($C_{10}H_9$), 2.78–0.71 (C_2H_2); ^{13}C NMR ($CDCl_3$, *δ/ppm*): 133.7 (C_2H_3), 111.7 (C_2H_3), 69.5–67.8 (^{t}C-C_5H_3), 67.6–66.1 (C_5H_3), 65.5–64.3 (C_5H_4), 32.1 (C_2H_3), 29.8 (C_2H_3), 22.6 (C_2H_3), 14.3 (C_2H_3); IR (KBr, cm^{-1}): 3082 (m), 2920 (m), 2853 (m), 1624 (m), 1455 (m), 982 (s), 892 (m), 799 (s).

*2.7.2.4. Synthesis of poly(-1,1′,2,2′-tetravinylferrocene) (**PVF-4s**).* 1,1′,2,2′-tetravinylferrocene **4** (1.0 eq, 1.50 g, 5.2 mmol), ^{n}BuLi (0.01 eq, 2.5 M in hexane, 20.68 mmL, 51.7 μmol). Product: 1.25 g, 82.2% as black powder; MALDI-TOF ($g \cdot mol^{-1}$): 856 (D = 1.05); elemental analysis calculated for $((C_{18}H_{18}Fe)_n \cdot (C_4H_9)_{0.01n})$ (290.82 g $mol^{-1})_n$: C, 74.50; H, 6.27. Found: C, 74.85; H, 7.55; ^{1}H NMR ($CDCl_3$, *δ/ppm*): 6.54–6.40 (C_2H_3), 5.42–4.95 (C_2H_3), 4.54–3.55 ($C_{10}H_9$), 2.77–0.68 (C_2H_2); ^{13}C NMR ($CDCl_3$, *δ/ppm*): 133.6 (C_2H_3), 112.9 (C_2H_3), 69.6–68.0 (^{t}C-C_5H_3), 67.8–66.1 (C_5H_3), 65.3–63.9 (C_5H_3), 31.9 (C_2H_3), 29.7 (C_2H_3), 22.5 (C_2H_3), 14.1 (C_2H_3); IR (KBr, cm^{-1}): 3083 (m), 2924 (m), 2854 (m), 1625 (m), 1453 (m), 981 (s), 892 (m), 799 (s).

*2.7.2.5. Synthesis of poly(vinylferrocene-co-1,2-divinylferrocene) (**PVF-5s**).* Vinylferrocene **1** (1.0 eq, 1.50 g, 7.1 mmol, 1,2-divinylferrocene **2** (0.1 eq, 0.17 g, 0.07 mmol), ^{n}BuLi (0.01 eq, 2.5 M in hexane, 31.1 mmL, 77.8 μmol). Product: 1.35 g, 80.8% as yellow powder; MALDI-TOF ($g \cdot mol^{-1}$): 2020 (D = 1.17); elemental analysis calculated for $((C_{12}H_{12}Fe)_n \cdot (C_{12}H_{12}Fe)_{0.1n})$ (235.87 g $mol^{-1})_n$: C, 68.2; H, 5.70. Found: C, 66.58; H, 5.86; ^{1}H NMR ($CDCl_3$, *δ/ppm*): 6.51–6.37 (C_2H_3), 5.41–4.97 (C_2H_3), 4.57–3.55 ($C_{10}H_9$), 3.04–0.67 (C_2H_2); ^{13}C NMR ($CDCl_3$, *δ/ppm*): 69.9 (^{t}C-C_5H_4), 69.4 (^{t}C-C_5H_3), 68.6 (C_5H_4, C_5H_3), 67.1 (C_5H_5) 32.5 (C_2H_3), 32.4 (C_2H_3), 23.0 (C_2H_3), 14.3 (C_2H_3); IR (KBr, cm^{-1}): 3092 (m), 2925 (m), 2857 (m), 1629 (m), 1459 (m), 1411 (m), 1336 (m), 999 (s), 814 (s).

*2.7.2.6. Synthesis of poly(vinylferrocene-co-1,1′,2-trivinylferrocene) (**PVF-6s**).* Vinylferrocene **1** (1.0 eq, 1.50 g, 7.1 mmol), 1,1′,2-trivinylferrocene **3** (0.1 eq, 0.19 g, 0.07 mmol), ^{n}BuLi (0.01 eq, 2.5 M in hexane, 31.1 mmL, 77.8 μmol). Product: 1.38 g, 81.7% as yellow powder; MALDI-TOF ($g \cdot mol^{-1}$): 2179 (D = 1.19); elemental analysis calculated for $((C_{12}H_{12}Fe)_n \cdot (C_{16}H_{16}Fe)_{0.1n})$ (238.48 g $mol^{-1})_n$: C, 68.5; H, 5.80. Found: C, 68.30; H, 6.20; ^{1}H NMR ($CDCl_3$, *δ/ppm*): 6.72–6.30 (C_2H_3), 5.59–4.92 (C_2H_3), 4.85–3.03 ($C_{10}H_9$), 2.88–0.19 (C_2H_2); ^{13}C NMR ($CDCl_3$, *δ/ppm*): 134.8 (C_2H_3), 111.2 (C_2H_3), 69.3 (^{t}C-C_5H_4), 68.8 (^{t}C-C_5H_3), 68.6 (C_5H_4, C_5H_3), 67.1 (C_5H_5), 66.8 (C_5H_5), 32.1 (C_2H_3), 29.8 (C_2H_3), 22.9 (C_2H_3), 14.3 (C_2H_3); IR (KBr, cm^{-1}): 3090 (m), 2924 (m), 2849 (m), 1626 (m), 1460 (m), 1411 (m), 1336 (m), 1000 (s), 814 (s).

*2.7.2.7. Synthesis of poly(vinylferrocene-co-1,1′,2,2′-tetravinylferrocene) (**PVF-7s**).* Vinylferrocene **1** (1.0 eq, 1.50 g, 7.1 mmol), 1,1′,2,2′-tetravinylferrocene **4** (0.1 eq, 0.21 g, 0.07 mmol), ^{n}BuLi (0.01 eq, 2.5 M in hexane, 31.1 mmL, 77.8 μmol). Product: 1.39 g, 80.7% as brownish-yellow powder; MALDI-TOF ($g \cdot mol^{-1}$): 2285 (D = 1.23); elemental analysis calculated for $((C_{12}H_{12}Fe)_n \cdot (C_{18}H_{18}Fe)_{0.1n})$ (241.09 g $mol^{-1})_n$: C, 68.7; H, 5.80. Found: C, 67.59; H, 6.25; ^{1}H NMR ($CDCl_3$, *δ/ppm*): 7.20–7.05 (C_2H_3), 5.48–5.16 (C_2H_3), 4.67–3.41 ($C_{10}H_9$), 2.69–0.47 (C_2H_2); ^{13}C NMR ($CDCl_3$, *δ/ppm*): 134.8 (C_2H_3), 111.2 (C_2H_3), 69.3 (^{t}C-C_5H_4), 68.8 (C_5H_4), 68.5 (C_5H_2), 67.1 (C_5H_5), 66.8 (C_5H_5), 32.3 (C_2H_3), 29.8 (C_2H_3), 22.8 (C_2H_3), 14.3 (C_2H_3); IR (KBr, cm^{-1}): 3088 (m), 2924 (m), 2853 (m), 1625 (m), 1456 (m), 1411 (m), 1340 (m), 1000 (s), 814 (s).

3. Results and discussion

3.1. Synthesis

Polyvinylferrocene **PVF-1s** (**s** denotes polymerization in solution; **b** denotes polymerization in bulk) is accessible by anionic polymerization at room temperature of vinylferrocene **1** in tetrahydrofuran (15 mL $mmol^{-1}$) using ^{n}BuLi as the initiator (conditions deviate from previous reports [39–41] [45]) (Scheme 1), This methodology allowed for a high monomer conversion and low dispersities (D = $\overline{M}_w/\overline{M}_n$) of polyvinylferrocenes. In addition copolymerization of **1** with multivinylferrocenes (1,2-divinylferrocene **2** [64], 1,1′,2-trivinylferrocene **3** or 1,1′,2,2′-tetravinylferrocene **4**) [52] were polymerized (Scheme 1) and used to generate cross-linked copolymer PVFs with a varying degree of branching (**PVF-5s**, **PVF-6s**, **PVF-7s**) (Scheme 2) in very good yields. Furthermore, since vinylferrocenes **1**–**4** are low melting materials solvent free bulk polymerization at 70 °C was performed using ^{n}BuLi as initiator giving polyvinylferrocene **PVF-1b** (Scheme 1), cross-linked **PVF-2b**, **PVF-3b** and **PVF-4b**, respectively (Scheme 1) as well as copolymers **PVF-5b**, **PVF-6b** and **PVF-7b** (Scheme 2) in high yields and relatively high dispersity. The bulk reaction was found to progress much faster as complete monomer conversion has been observed over the course of less than 10 min. While the PVFs from solution polymerization (**PVF-1s** – **PVF-7s**) are soluble in most common organic solvents (e.g., dichloromethane, toluene and tetrahydrofuran), the highly cross-linked polymers **PVF-3b**, **PVF-4b, PVF-6b** and **PVF-7b** are insoluble. This difference in the behavior points to the fact that the cross-linking units are better incorporated during the polymerization process within the bulk reaction compared with the appropriate solution protocol, and hence the degree of branching increases. Furthermore, post-reaction workup showed no presence of monomeric material demonstrating full conversion of the polymerization reaction in bulk, hence in combination with the cross-linking high molecular masses are expected.

3.2. Characterization

All PVFs are solid materials at 25 °C (yellow: (**PVF-(1s – 7s)**, **PVF-1b**, **PVF-2b**, **PVF-5b**), (brown: **PVF-6b**, **PVF-7b**) (dark brown: **PVF-3b**, **PVF-4b**). The PVFs were characterized by MALDI-TOF mass spectrometry, elemental analysis, IR-, *in situ*-UV/Vis-NIR- and NMR-spectroscopy (^{1}H, ^{13}C{^{1}H}), solid state NMR spectroscopy (^{1}H-MAS, ^{13}C{^{1}H} CP-MAS), as well as electrochemical measurements.

The MALDI-TOF mass spectra of **PVF-1b** and **PVF-1s** show that bulk polymerization led to a higher average molar mass and D when compared to PVFs obtained from anionic polymerization in solution (Fig. 1). Polymerization of 1,2-divinylferrocene **2** results in polymers with additional vinyl functionalities which offer the possibility of cross-linking. Within the MALDI-TOF results of **PVF-2s**, the trend that the bulk polymerization produces longer polymer chains is confirmed (see Supporting information Table SI1). Furthermore, the MALDI-TOF mass spectra of **PVF-2b** show two major distributions with a $\Delta(m/z) = 56$ which is the result of the initiation by either a butyl anion or a hydride ion. The higher polymerization temperature of 70 °C may be responsible for the decomposition of the used ^{n}BuLi, and hence, hydride ions are available to initiate the polymerization. However, chain transfer reactions during the polymerization may also be responsible for this molecular mass distribution.

Unfortunately, for highly cross-linked **PVF-3(b, s)** and **PVF-4(b, s)** no reliable MALDI-TOF spectra could be obtained, as cross-linked polymers are notoriously hard to efficiently ionize and desorp from the matrix in the MALDI process. In addition, for polymers of **PVF-5** – **PVF-7(b, s)** the MALDI spectra showed only moderate chain length which might reflect fragmentation during the ionization prozess and, hence, the spectra posses only limited information about the whole material. However, the presence of multifunctional monomers **2**, **3** or **4** in the co-polymers with vinylferrocene **1** was proven by MALDI-TOF measurements. While it was found that under our experimental conditions a fraction of the polymeric mixture always contains non-cross-linked PVFs, series of polymer chains with different number of incorporated cross-linking units are also present. The one, two or three additional vinyl functionalities are represented by individual signal patterns with

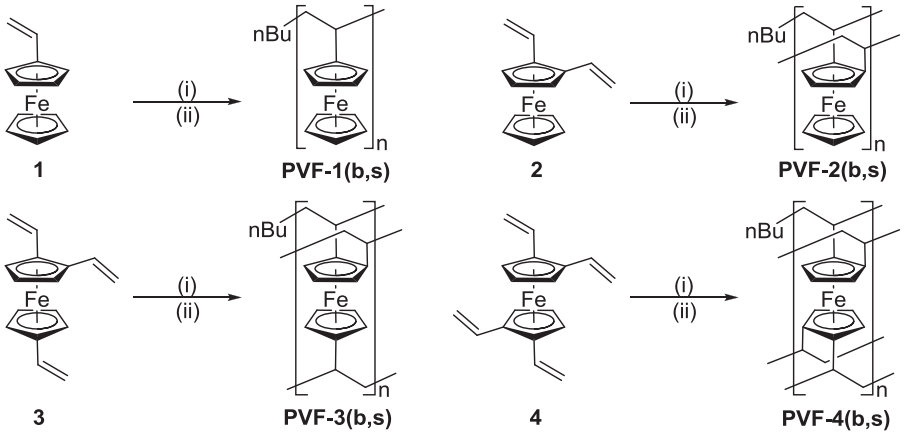

Scheme 1. Anionic polymerization of vinylferrocenes to linear and cross-linked polyvinylferrocenes (PVFs). (b = in bulk, s = in solution). (i) for bulk route: 1st: 70 °C, 1 min; 2nd: ^{n}BuLi (0.01 eq), 2 min; 3rd: anhydrous toluene (0.15 mL/1 mmol), 1 h; for solution route: 1st: tetrahydrofuran (15 mL/1 mmol), 25 °C; 2nd: ^{n}BuLi (0.01 eq), 2 h (ii) methanol (1 eq.), 15 min.

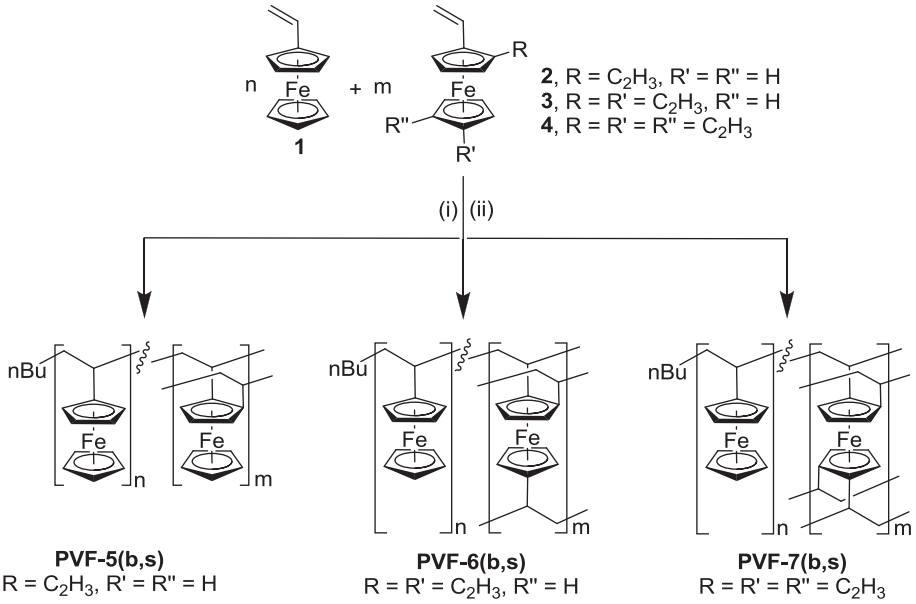

Scheme 2. Co-polymerization of vinylferrocene **1** with multifunctional vinylferrocenes **2**, **3** or **4** as cross-linker. (b = in bulk, s = in solution). (i) for bulk route: 1st: 70 °C, 1 min; 2nd: ^{n}BuLi (0.01 eq), 2 min; 3rd: anhydrous toluene (0.15 mL/1 mmol), 1 h; for solution route: 1st: tetrahydrofuran (15 mL/1 mmol), 25 °C; 2nd: ^{n}BuLi (0.01 eq), 2 h (ii) methanol (1 eq.), 15 min.

differences of $\Delta(m/z) = 26$, 52 and 76 from the polyvinylferrocene peaks (Fig. 2). For these series it is shown that polymers containing a higher number of the cross-linking units **2**–**4** exhibit lower D value as well as a higher average molar masses, both for the polymerization in solution and bulk. For compound **PVF-7b** only polymer fragments were found in which the tetravinylferrocene motive is present once per polymeric chain, probably because of the MALDI-TOF detection limit.

The IR spectra of polymers **PVF-1b** and **PVF-1s** show that the vinyl stretching vibrations at 3081 cm^{-1} ν(=C-H stretching) and 1628 cm^{-1} ν(C=C stretching) [65] disappear after the living anionic polymerization for compound **1**. The appearance of ν(-C-H) bands (**PVF-1b**: 2925 cm^{-1}, 2852 cm^{-1} ν(-C-H stretching), 1461 cm^{-1} δ(-C-H bending), 1339 cm^{-1} δ(-C-H rocking); **PVF-1s**: 2928 cm^{-1}, 2847 cm^{-1} ν(-C-H stretching), 1458 cm^{-1} δ(-C-H bending), 1336 cm^{-1} δ(-C-H rocking)) confirm the of the anionic polymerization. Within the IR measurements, the same individual signal pattern for the cross-linked polymers **PVF-2** – **PVF-4(b, s)** were found. In addition, due to incomplete conversion of all vinyl groups in case of the highly functionalized ferrocene **3** and **4** [52], the = C-H bending bands are shifted from 899 cm^{-1} and 894 cm^{-1} in **3** and **4**–895 cm^{-1} and 892 cm^{-1} in **PVF-3(b,s)** and **PVF-4(b,s)**, respectively. The vinylferrocene co-polymers **PVF-5** – **PVF-7(b,s)** show the same IR characteristic as the solely cross-linked polymers.

In general, broad peaks in the ^{1}H NMR are observed, which is typical for polymer compounds. The individual ferrocenyl signals are superimposed and are reflected by one multiplet signal in the spectral region of 3.2–4.9 ppm. In addition aliphatic protons of the CH_2 and CH groups are found as broad signal at 0.2–3.0 ppm. For the linear polymers **PVF-1b** and **PVF-1s** solely these pattern were found. The cross-linked co-polymers show two additional weak signals in the spectral region between 5.2 and 7.0 ppm, which are attributed to the unconverted vinyl functionalities. Since the highly cross-linked polymers **PVF-2b**, **PVF-3b**, **PVF-4b** and **PVF-7b** are

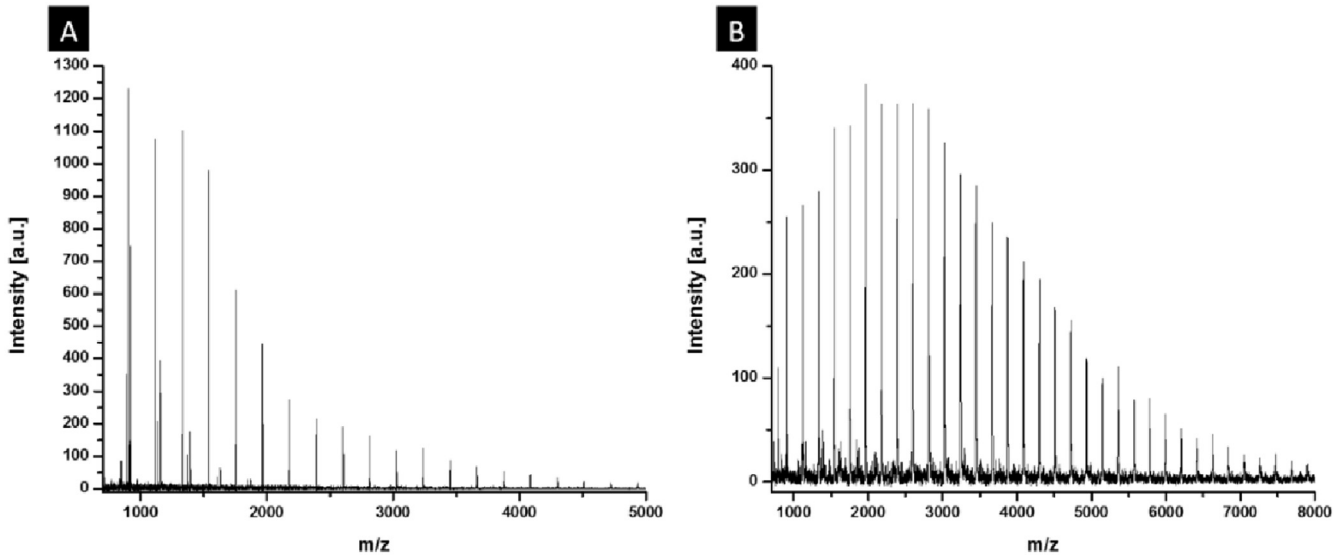

Fig. 1. MALDI-TOF mass spectra; (**A**) for **PVF-1s**, (**B**) for **PVF-1b**.

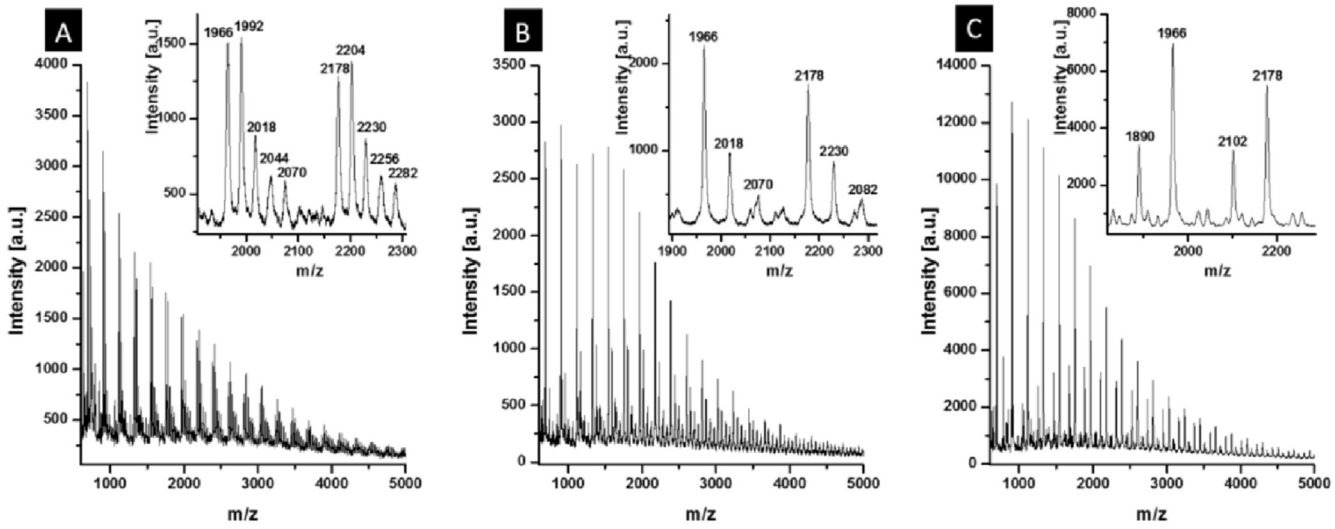

Fig. 2. MALDI-TOF mass spectra; (**A**) for **PVF-5b**, (**B**) for **PVF-6b**, (**C**) for **PVF-7b**.

insoluble, solid state NMR studies have been performed. In the solid state NMR measurements the presence of ferrocenyl functionalities (around 4.1 ppm) as well as the ethylene moieties (around 1.2 ppm) are identified. Furthermore, the unconverted vinyl functionalities are indicated by the presence of very weak signals (around 7.1 ppm). However, due to the broad peak width, no further details were accessible. Within solution ^{13}C NMR spectra, polymers **PVF-1b** and **PVF-1s** show individual signals for the ferrocenyl moieties in the spectral region between 64 and 97 ppm and resonances for the aliphatic carbon atoms between 14 and 35 ppm. The cross-linked polymers (**PVF-(2s – 4s)**) as well as the co-polymers (**PVF-5(b,s)** and **PVF-6(b,s)**) show two additional peaks between 110 and 135 ppm attributed to the presence of unconverted vinyl functionalities.

The ferrocenyl signals were observed in a more narrow spectral region between 66 and 71 ppm, while the CH_2- signals are detected between 14 and 45 ppm. Solid state ^{13}C NMR of (**PVF-(2b – 4b)**) and co-polymers (**PVF-7(b,s)**) demonstrated signals for the unconverted vinyl functionalities in the spectral region between 110 and 135 ppm, ferrocenyl units between 69 and 100 ppm and the CH_2-aliphatic between 15 and 45 ppm.

3.3. Electrochemistry and spectroelectrochemistry

The electro-chemical behavior of **PVF-(1s – 7s)** was investigated by cyclic voltammetry, square wave voltammetry and spectroelectrochemistry using 0.1 mol L^{-1} anhydrous dichloromethane solutions of $[N^nBu_4][B(C_6F_5)_4]$ as supporting electrolyte [52–58]. The electrochemical measurements were carried out at 25 °C, and were referenced against the potential of the FcH/FcH^+ redox couple [59].

Exemplary, the cyclic voltammograms of polyvinylferrocenes **PVF-1s** and co-polymer **PVF-5s** are depicted in Fig. 3 and are summarized in Table 1. The cyclic voltammograms of the other compounds are found as Figures SI-(1–5) in the supporting information. For all polymeric materials a reversible redox behavior was observed. However, due to the polymeric nature of the compounds, the signals of several ferrocenyl-related oxidations are

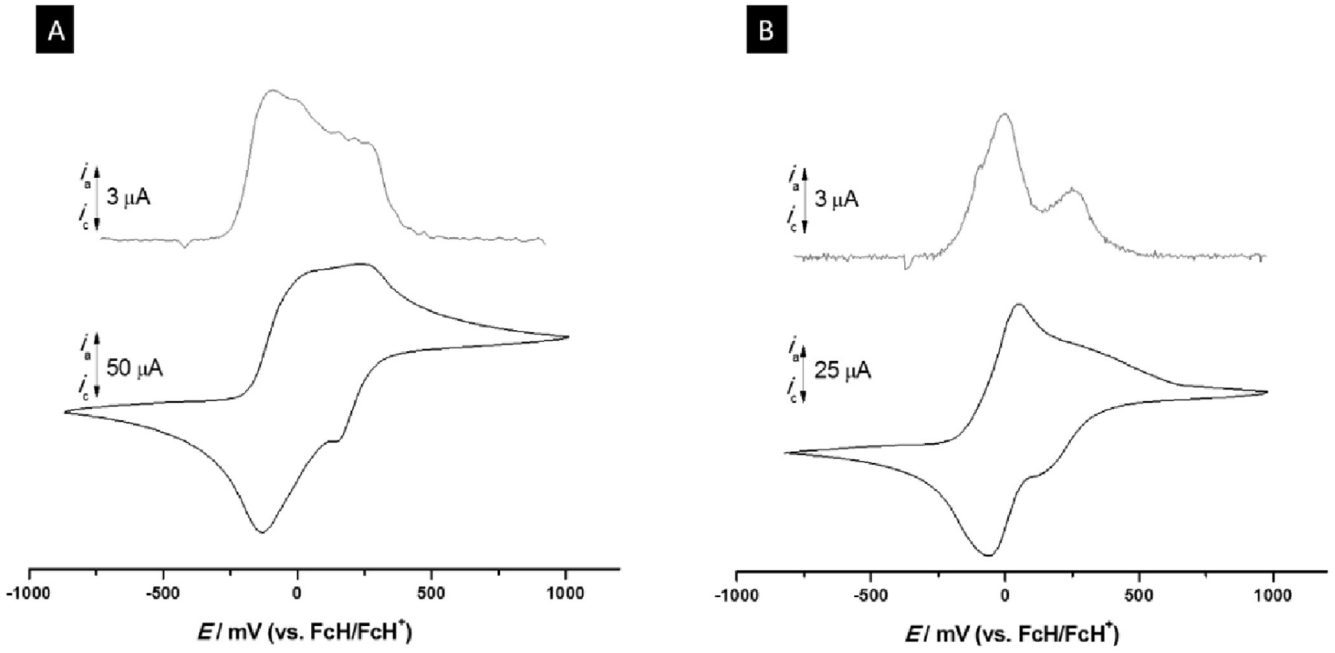

Fig. 3. Voltammograms of anhydrous dichloromethane solution of (**A**) **PVF-1s** (0.5 mmol L^{-1}) (**B**) **PVF-5s** (0.5 mmol L^{-1}), ($[N^nBu_4][B(C_6F_5)_4]$ (1.0 mmol L^{-1}) used as electrolyte) at 25 °C: (bottom) cyclic voltammogram, (top) square wave voltammogram.

Table 1
Cyclic voltammetry data of polymers **PVF-**(**1s** – **7s**).

Compound	E(Onset)[a] in mV	E(Offset)[b] in mV
PVF-1s	−244	410
PVF-2s	−300	461
PVF-3s	−330	470
PVF-4s	−340	515
PVF-5s	−222	428
PVF-6s	−248	445
PVF-7s	−260	486

[a] E(Onset): start of differential current increase for the first ferrocenyl based oxidation as determined by SWV.
[b] E(Offset): end of the oxidation processes as determined by SWV.

superimposed with each other. For compound **PVF-1s** the oxidation of the ferrocenyl units starts at a potential of -250 mV *vs.* FcH/FcH^+ and the compound is fully oxidized at 400 mV. The aliphatic CH_2-CH- bridging moiety acts as electron donor towards the ferrocenyl functionalities and, hence, the first oxidation is shifted by approx. 250 mV towards more positive potentials with respect to ferrocene. For all PVFs two maxima in the electrochemical measurements are found which reflects the fact that at more negative potentials every second ferrocenyl unit oxidizes and hence, increases the electrostatic interactions between the Fe^{3+} ions leading to a further signal shift up to 400–500 mV where all ferrocenyl groups are oxidized to ferrocenium functionalities. Due to the reduced ion pairing capabilities of the weakly coordinating electrolyte ($[N^nBu_4][B(C_6F_5)_4]$) in comparison to classical electrolytes such as PF_6^- or halides, these electrostatic effects are not shielded and a potential difference between the ferrocenyl oxidations can be observed [54]. Multicyclic experiments showed stable ferrocenyl/ferrocenium redox couples for these polymers for at least up to 100 cycles (see Figures SI-(6–13)). However, it is not possible to assign individual redox events to certain processes.

In-situ-UV/Vis-NIR spectroelectrochemical measurements of **PVF-**(**1s** – **7s**) allowed to determine electron transfer processes between the individual ferrocenyl units in the polymer chains. While typical ligand-to-metal charge transfer (LMCT) excitations of the cyclopentadienyls towards the Fe^{3+} ions are found upon oxidation, no intervalence charge transfer (IVCT) band was detected (Fig. 4, Figure SI-(13–18) within the supporting information). This contrast examples of "main chain" ferrocene polymers in which electron transfer excitations can be observed [50] [66].

The aliphatic character of the connecting units between the ferrocenyl hinders a through-bond metal-metal coupling along the chains. However, such ferrocenyl-containing polymers can exhibit notable conductivity due to electron hopping mechanisms between the individual chains [50]. [66–70].

In order to evaluate the possible application as cathode material in Li-ion batteries solid state electrochemical measurements have been carried out in Swagelok test cells using a lithium foil counter electrode and a Whatman glass fiber separator (see experimental part).

In accordance to the electrochemical measurements in solution polyvinylferrocene compounds **PVF-1b** and **PVF-**(**5b** – **7b**) showed a reversible redox behavior (see Figures SI-(19–22)). The reduction as well as the oxidation reaction become increasingly defined with growing degree of cross-linking in the respective polymer. This behavior is reflected in the decreasing signal width at half height and continuously growing peak current with increasing degree of cross-linking. These observations are attributed to the decreasing solubility of the cross-linked polymers and an increased swelling behavior which is usually observed in highly cross-linked polymers. In turn, a swollen polymeric active material can facilitate ion transport and electrolyte accessibility of the redox active ferrocene centers. In addition the ferrocene-based active materials display a nominal cell voltage of around 3.2 V which is comparable to standard Li-ion cathode materials like $LiFePO_4$ with 3.45 V [23].

Galvanostatic cycling experiments show high initial discharge capacities for **PVF-1b** (76 $mAh \cdot g^{-1}_{PVF}$), **PVF-6b** (79 $mAh \cdot g^{-1}_{PVF}$) and **PVF-7b** (80 $mAh \cdot g^{-1}_{PVF}$) while the initial discharge capacity of **PVF-5b** only reaches up to 59 $mAh \cdot g^{-1}_{PVF}$. The cycling stability of the polyvinylferrocenes is also strongly affected by the degree of cross-linking (Fig. 5). While the discharge capacity of the solely

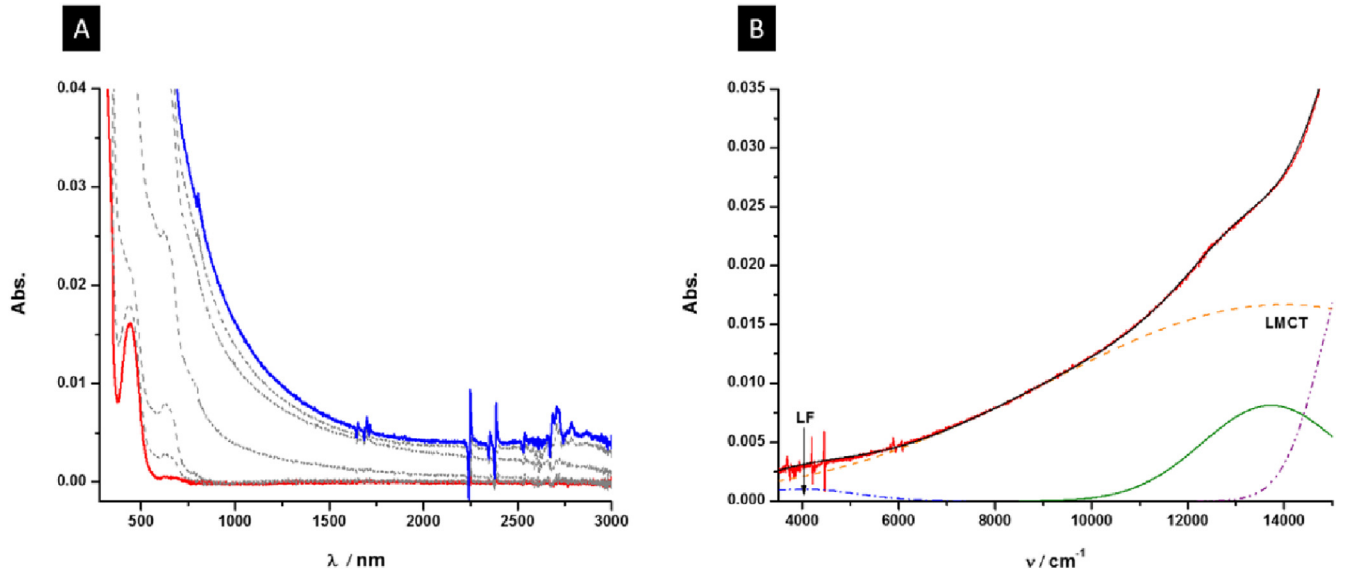

Fig. 4. (**A**) UV/Vis-NIR spectra of **PVF-6s** at 25° C in anhydrous dichloromethane (0.25 mmol L^{-1}) at increasing potentials (bottom, −200 (red line) to 1600 mV (blue line) vs Ag/AgCl); supporting electrolyte $[N^nBu_4][B(C_6F_5)_4]$. (**B**) Deconvolution of the near-IR absorptions of $[\textbf{PVF-6s}]^{n+}$ using three Gaussian-shaped bands determined by spectroelectrochemistry in an OTTLE cell; red line: experimental data; black dotted line: simulated spectra.

linear **PVF-1b** and the sparsely cross-linked **PVF-5b** drops below 40 $mAh \cdot g^{-1}_{PVF}$ after 40 charge/discharge cycles. The highest cross-linked **PVF-7b** displays, after a few forming cycles, a stable discharge capacity of 90 $mAh \cdot g^{-1}_{PVF}$ (Fig. 5). From this specific capacity an energy density of 290 $Wh \cdot kg^{-1}$ is calculated. The herein reported ferrocene-based polymeres show comparable results for lithium storage as found for other polymer systems in literature [37]. [48].

In addition, ferrocene and derived compounds are discussed as serious candidates for sustainable redox-flow battery catholytes [51]. [71,72].

4. Conclusion

Bulk and solution anionic polymerization methodologies have been used to polymerize mono-vinylferrocene **1** and multifunctional ferrocenes bearing two to four vinyl groups **2**, **3**, **4** into giving linear polyvinylferrocene **PVF-1**(**b**, **s**), cross-linked **PVF-2** – **PVF-4**(**b**, **s**) and co-polymers **PVF-5** – **PVF-7**(**b**, **s**). The polymerization in bulk afforded **PVF-**(**1b** – **7b**) with high monomer consumption and a relatively high dispersity = D when compared with the PVFs obtained by anionic polymerization in solution **PVF-**(**1s** – **7s**). The polymers have been characterized by MALDI-TOF mass spectrometry, IR-, NMR- (^{1}H, ^{13}C{^{1}H}) (**PVF-**(**1s** – **7s**), **PVF-**(**1b**, **5b**)) and solid state NMR spectroscopy (^{1}H-MAS, ^{13}C{^{1}H} CP-MAS) (**PVF-**(**2**–**4**, **6**, **7**)**b**) as well as *in-situ*-UV/Vis-NIR spectroelectrochemistry and cyclic voltammetry **PVF-**(**1s** – **7s**). It is noticeable that the polymerization in bulk protocol leads to longer polymer chains. Polymer materials **PVF-**(**1s** – **7s**) are found to be soluble in the most common organic solvent such as DCM, THF and toluene. As expected, cross-linked **PVF-3b**, **PVF-4b**, **PVF-6b** and **PVF-7b** are poorly soluble or insoluble. We showed that the degree of branching is higher for PVFs obtained in bulk polymerization which demonstrates that the cross-linkers are better incorporated into the polymer. The co-polymerization process of vinylferrocene **1** and vinylferrocenes **2**, **3**, **4** are proven by the MALDI-TOF spectra of **PVF-5** – **PVF-7**(**b**, **s**) due to the presence of an individual signal patterns with $\Delta(m/z)$ = 26, 52 and 76 originating from polyvinylferrocene peaks.

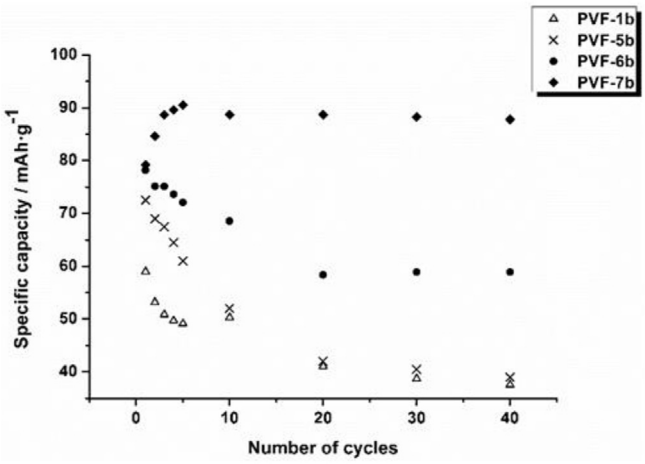

Fig. 5. Specific discharge capacity of the PVFs (**PVF-1b** and **PVF-**(**5b** – **7b**).

In the electrochemical measurements, reversible redox behavior for the polymers **PVF-**(**1s** – **7s**) are observed. The shift of the first oxidation process towards more positive potentials (from -250 mV to approx. 250 mV *vs.* Fc) hints to electron donor activity of the aliphatic bridging moiety towards the ferrocenyl functionalities. Furthermore, the ferrocenyl/ferrocenium redox couples are stable for at least 100 cycles for all polymers. Due to different types of monomer building blocks in the co-polymers **PVF-**(**5s** – **7s**), the materials are oxidized at different potentials and two distinct maxima within the square wave voltammetry measurements were observed. From the results of the *in-situ*-UV/Vis-NIR spectroelectrochemistry on all polymeric materials **PVF-**(**1s** – **7s**) no IVCT band was found. A hindered metal-metal communication along the chains related to the aliphatic units between the ferrocenyl units is reasoned for this observation. LMCT excitations were found upon oxidation caused by the interaction of Fe^{3+} ions with the cyclopentadienyl group.

The applicability of polyvinyl ferrocenes **PVF-1b** and **PVF-(5b** – **7b)** as cathode material was demonstrated by lithium ion battery

cell tests, showing that the highest cross linked co-polymer **PVF-7b** achieved a stable discharge capacity of 90 $mAh \cdot g^{-1}_{PVF}$ calculated to an energy density of 290 $Wh \cdot kg^{-1}_{PVF}$.

Acknowledgements

We are very grateful to Prof. Dr. Heinrich Lang for the supply of laboratory space and equipment.

Appendix A. Supplementary data

Supplementary data related to this article can be found at https://doi.org/10.1016/j.jorganchem.2017.10.009.

References

[1] I. Manners, Synthetic Metal-containing Polymers, WILEY-VCH, Weinheim, Germany, 2004.
[2] B.J. Holliday, T.M. Swager, Conducting metallopolymers: the roles of molecular architecture and redox matching, Chem. Commun. (2005) 23–36, https://doi.org/10.1039/b408479a.
[3] C. Engtrakul, L.R. Sita, Ferrocene-based nanoelectronics: 2,5-diethynylpyridine as a reversible switching element, Nano Lett. 1 (2001) 541–549, https://doi.org/10.1021/nl010038p.
[4] T.J. Kealy, P.L. Pauson, A new type of organo-iron compound, Nature 168 (1951) 1039–1040, https://doi.org/10.1038/1681039b0.
[5] K. Heinze, H. Lang, Ferrocene - beauty and function, Organometallics 32 (2013) 5623–5625, https://doi.org/10.1021/om400962w.
[6] R.W. Heo, T.R. Lee, Ferrocenophanes with all carbon bridges, J. Organomet. Chem. 578 (1999) 31–42, https://doi.org/10.1016/S0022-328X(98)01126-7.
[7] F.S. Arimoto, A.C. Haven Jr., Derivatives of dicyclopentadienyliron, J. Am. Chem. Soc. 77 (1955) 6295–6297, https://doi.org/10.1021/ja01628a068.
[8] J.C. Lai, T. Rounsfell, C.U. Pittman Jr., Free-radical homopolymerization and copolymerization of Vinylferrocene, J. Polym. Sci. Part A-1 9 (1971) 651–662, https://doi.org/10.1002/pol.1971.150090307.
[9] R.D.A. Hudson, Ferrocene polymers: current architectures, syntheses and utility, J. Organomet. Chem. 637–639 (2001) 47–69, https://doi.org/10.1016/S0022-328X(01)01142-1.
[10] K. Kulbaba, I. Manners, Polyferrocenylsilanes: metal-containing polymers for materials science, self-assembly and nanostructure applications, Macromol. Rapid Commun. 22 (2001) 711–724, https://doi.org/10.1002/1521-3927(20010701)22:10<711::AID-MARC711>3.0.CO;2-C.
[11] C.G. Hardy, L. Ren, T.C. Tamboue, C. Tang, Side-chain ferrocene-containing (Meth)acrylate polymers: synthesis and properties, J. Polym. Sci. Part A Polym. Chem. 49 (2011) 1409–1420, https://doi.org/10.1002/pola.24561.
[12] D.A. Foucher, B.Z. Tang, I. Manners, Ring-opening polymerization of strained, ring-tilted ferrocenophanes: a route to high-molecular-weight poly(-ferrocenylsilanes), J. Am. Chem. Soc. 114 (1992) 6246–6248, https://doi.org/10.1021/ja00041a053.
[13] T. Morikita, T. Yamamoto, Electrochemical determination of diffusion coefficient of π-conjugated polymers containing ferrocene unit, J. Organomet. Chem. 637–639 (2001) 809–812, https://doi.org/10.1016/S0022-328X(01)00941-X.
[14] C. Su, Y. Ye, L. Xu, C. Zhang, Synthesis and charge–discharge properties of a ferrocene-containing polytriphenylamine derivative as the cathode of a lithium ion battery, J. Mater. Chem. 22 (2012) 22658–22662, https://doi.org/10.1039/c2jm34752k.
[15] H. Zhong, G. Wang, Z. Song, X. Li, H. Tang, Y. Zhou, et al., Organometallic polymer material for energy storage, Chem. Commun. 50 (2014) 6768–6770, https://doi.org/10.1039/c4cc01572j.
[16] C. Su, L. Wang, L. Xu, C. Zhang, Synthesis of a novel ferrocene-contained polypyrrole derivative and its performance as a cathode material for Li-ion batteries, Electrochim. Acta 104 (2013) 302–307, https://doi.org/10.1016/j.electacta.2013.04.127.
[17] Y. Tang, X. Zeng, Poly(Vinyl ferrocene) redox behavior in ionic liquids, J. Electrochem. Soc. 155 (2008) 82–90, https://doi.org/10.1149/1.2868797.
[18] R. Sun, L. Wang, H. Yu, Z. Abdin, Y. Chen, J. Huang, et al., Molecular recognition and sensing based on ferrocene derivatives and ferrocene-based polymers, Organometallics 33 (2014) 4560–4573, https://doi.org/10.1021/om5000453.
[19] B.W. Cadson, L.L. Miller, P. Neta, J. Grodkowski, Oxidation of NADH involving rate-limiting one-electron transfer, J. Am. Chem. Soc. 106 (1984) 7233–7239, https://doi.org/10.1021/ja00335a062.
[20] J. Elbert, M. Gallei, C. Rüttiger, A. Brunsen, H. Didzoleit, B. Stühn, et al., Ferrocene polymers for switchable surface wettability, Organometallics 32 (2013) 5873–5878, https://doi.org/10.1021/om400468p.
[21] J. Morsbach, A. Natalello, J. Elbert, S. Winzen, A. Kroeger, H. Frey, et al., Redox-responsive block copolymers: poly(vinylferrocene)-b-poly(lactide) diblock and miktoarm star polymers and their behavior in solution, Organometallics 32 (2013) 6033–6039, https://doi.org/10.1021/om400536q.
[22] X. Su, K. Tan, J. Elbert, C. Rüttiger, M. Gallei, T.F. Jamison, et al., Asymmetric Faradaic systems for selective electrochemical separations, Energy Environ. Sci. 10 (2017) 1272–1283, https://doi.org/10.1039/C7EE00066A.
[23] K.-Y. Hou, A. Rehman, X. Zeng, Study of ionic liquid immobilization on polyvinyl ferrocene substrates for gas sensor arrays, Langmuir 27 (2011) 5136–5146, https://doi.org/10.1021/la104191n.
[24] F. Dursun, S.K. Ozoner, A. Demirci, M. Gorur, F. Yilmaz, E. Erhan, Vinylferrocene copolymers based biosensors for phenol derivatives, J. Chem. Technol. Biotechnol. 87 (2012) 95–104, https://doi.org/10.1002/jctb.2688.
[25] Y. Li, M. Josowicz, L.M. Tolbert, Diferrocenyl molecular wires. The role of heteroatom linkers, J. Am. Chem. Soc. 132 (2010) 10374–10382, https://doi.org/10.1021/ja101585z.
[26] A. Greiner, B. Bolle, P. Hesemann, J.M. Oberski, R. Sander, Preparation and structure-property relationships of polymeric materials containing arylene-vinylene segments—perspectives for new light-emitting materials, Macromol. Chem. Phys. 197 (1996) 113–134, https://doi.org/10.1002/macp.1996.021970109.
[27] R.A. Dvorikova, L.N. Nikitin, Y.V. Korshak, V.A. Shanditsev, A.L. Rusanov, S.S. Abramchuk, et al., New magnetic nanomaterials based on hyperbranched ferrocene-containing polyphenylenes synthesized in sub-and supercritical carbon dioxide, Dokl. Chem. 422 (2008) 231–235, https://doi.org/10.1134/S0012500808090085.
[28] J.S. Miller, A.J. Epstein, W.M. Reiff, Ferromagnetic molecular charge-transfer complexes, Chem. Rev. 88 (1988) 201–220, https://doi.org/10.1021/cr00083a010.
[29] A.E.W. Sarhan, Y. Nouchi, T. Izumi, Synthesis and electrochemical studies of ferrocene-dithiafulvalenes (Fc-DTF) and 1,1'-bis(dithiafulvalenyl)ferrocene (DTF-Fc-DTF). An approach towards new conducting organic materials, Tetrahedron 59 (2003) 6353–6362, https://doi.org/10.1016/S0040-4020(03)00951-7.
[30] A. Hildebrandt, K. Al Khalyfeh, J.F. Nawroth, R. Jordan, Electron transfer studies on conjugated ferrocenyl-containing oligomers, Organometallics 35 (2016) 3713–3719, https://doi.org/10.1021/acs.organomet.6b00673.
[31] M.D. McGehee, A.J. Heeger, Semiconducting (conjugated) polymers as materials for solid-state lasers, Adv. Mater. 12 (2000) 1655–1668. https://doi.org/10.1002/1521-4095(200011)12:22<1655::AID-ADMA1655>3.0.CO;2–2.
[32] R. Rulkens, R. Resendes, A. Verma, I. Manners, K. Murti, E. Fossum, et al., Ring-opening copolymerization of cyclotetrasilanes and silicon-bridged [1]Ferrocenophanes: synthesis and properties of polysilane-poly(ferrocenylsilane) random copolymers, Macromolecules 30 (1997) 8165–8171, https://doi.org/10.1021/ma9712662.
[33] T. Kawai, C. Iwakura, H. Yoneyama, Electrochemical characteristics of poly (vinylferrocene) derivatives for battery application, Electrochim. Acta 34 (1989) 1357–1361, https://doi.org/10.1016/0013-4686(89)85033-9.
[34] Y. Matsuura, K. Matsukawa, Electronic structures of ferrocene-containing polymers with heteroatom-bridges, Chem. Phys. Lett. 436 (2007) 224–227, https://doi.org/10.1016/j.cplett.2007.01.055.
[35] R. Gracia, D. Mecerreyes, Polymers with redox properties: materials for batteries, biosensors and more, Polym. Chem. 4 (2013) 2206–2214, https://doi.org/10.1039/c3py21118e.
[36] K.-S. Park, S.B. Schougaard, J.B. Goodenough, Conducting-polymer/Iron-redox-couple composite cathodes for lithium secondary batteries, Adv. Mater. 19 (2007) 848–851, https://doi.org/10.1002/adma.200600369.
[37] K. Tamura, N. Akutagawa, M. Satoh, J. Wada, T. Masuda, Charge/discharge properties of organometallic batteries fabricated with ferrocene-containing polymers, Macromol. Rapid Commun. 29 (2008) 1944–1949, https://doi.org/10.1002/marc.200800526.
[38] S.M. Beladi-Mousavi, S. Sadaf, L. Walder, M. Gallei, C. Rüttiger, S. Eigler, et al., Poly (vinylferrocene)– reduced graphene oxide as a high power/high capacity cathodic battery material, Adv. Energy Mater. 6 (2016), https://doi.org/10.1002/aenm.201600108, 1600108.
[39] V. Burkhardt, Synthese ferrocenhaltiger Polymere mit enger Molekulargewichtsverteilung, Dissertation, University of Bayreuth, Germany, 1992.
[40] O. Nuyken, V. Burkhardt, C. Hübsch, Anionic homo- and block copolymerization of vinylferrocene, Macromol. Chem. Phys. 198 (1997) 3353–3363, https://doi.org/10.1002/macp.1997.021981102.
[41] M. Gallei, R. Klein, M. Rehahn, Silacyclobutane-mediated re-activation of “sleeping” polyvinylferrocene macro-anions: a powerful access to novel metalloblock copolymers, Macromolecules 43 (2010) 1844–1854, https://doi.org/10.1021/ma902092j.
[42] T. Higashihara, R. Faust, Synthesis of novel block copolymers comprised of polyisobutylene and poly (vinylferrocene) segments, Macromolecules 40 (2007) 7453–7463, https://doi.org/10.1021/Ma070903d.
[43] F. Yan, T. Higashihara, R. Mosurkal, L. Li, K. Yang, R. Faust, et al., Self organization and redox behavior of poly(vinylferrocene)-block-poly(isobutylene)-block-poly(vinylferrocene) triblock copolymer, J. Macromol. Sci. Part A Pure Appl. Chem. 45 (2008) 911–914, https://doi.org/10.1080/10601320802380075.
[44] M. Baumert, J. Fröhlich, M. Stieger, H. Frey, R. Mülhaupt, H. Plenio, Styrene-vinylferrocene random and block copolymers by TEMPO-mediated radical polymerization, Macromol. Rapid Commun. 20 (1999) 203–209, https://doi.org/10.1002/(SICI)1521-3927(19990401)20:4<203::AID-MARC203>3.0.CO;2-I.
[45] J. Elbert, J. Mersini, N. Vilbrandt, C. Lederle, M. Kraska, M. Gallei, et al., Reversible activity modulation of surface-attached grubbs second generation type catalysts using redox-responsive polymers, Macromolecules 46 (2013)

4255–4267, https://doi.org/10.1021/ma4007126.
[46] T. Hirano, H.-S. Yoo, Y. Ozama, A.A. El-Magd, K. Sugiyama, A. Hirao, Precise synthesis of novel ferrocene-based star-branched polymers by using specially designed 1,1-diphenylethylene derivatives in conjunction with living anionic polymerization, J. Inorg. Organomet. Polym. Mater. 20 (2010) 445–456, https://doi.org/10.1007/s10904-010-9377-2.
[47] J. Morsbach, J. Elbert, C. Rüttiger, S. Winzen, H. Frey, M. Gallei, Polyvinylferrocene-based amphiphilic block copolymers featuring functional junction points for cross-linked micelles, Macromolecules 49 (2016) 3406–3414, https://doi.org/10.1021/acs.macromol.6b00514.
[48] J. Xiang, K. Sato, H. Tokue, K. Oyaizu, C.L. Ho, H. Nishide, et al., Synthesis and charge-discharge properties of organometallic copolymers of ferrocene and triphenylamine as cathode active materials for organic-battery applications, Eur. J. Inorg. Chem. (2016) 1030–1035, https://doi.org/10.1002/ejic.201501169.
[49] T.B. Issa, P. Singh, M.V. Baker, Potentiometric measurement of state-of-charge of lead-acid battery by using a bridged ferrocene surface modified electrode, J. Power Sources 158 (2006) 1034–1038, https://doi.org/10.1016/j.jpowsour.2005.11.034.
[50] W. Tian, X. Mao, P. Brown, G.C. Rutledge, T.A. Hatton, Electrochemically nanostructured polyvinylferrocene/polypyrrole hybrids with synergy for energy storage, Adv. Funct. Mater. 25 (2015) 4803–4813, https://doi.org/10.1002/adfm.201501041.
[51] H.-S. Kim, T. Yoon, Y. Kim, S. Hwang, J.H. Ryu, S.M. Oh, Increase of both solubility and working voltage by acetyl substitution on ferrocene for nonaqueous flow battery, Electrochem. Commun. 69 (2016) 72–75, https://doi.org/10.1016/j.elecom.2016.06.002.
[52] A. Hildebrandt, K. Al Khalyfeh, D. Schaarschmidt, M. Korb, Multi-functionalized ferrocenes: −Synthesis and characterization −, J. Organomet. Chem. 804 (2016) 87–94, https://doi.org/10.1016/j.jorganchem.2015.12.027.
[53] R.J. LeSuer, C. Buttolph, W.E. Geiger, Comparison of the conductivity properties of the tetrabutylammonium salt of tetrakis(pentafluorophenyl)borate anion with those of traditional supporting electrolyte anions in nonaqueous solvents, Anal. Chem. 76 (2004) 6395–6401, https://doi.org/10.1021/ac040087x.
[54] F. Barrière, W.E. Geiger, Use of weakly coordinating anions to develop an integrated approach to the tuning of $\Delta E_{1/2}$ values by medium effects, J. Am. Chem. Soc. 128 (2006) 3980–3989, https://doi.org/10.1021/ja058171x.
[55] J.C. Swarts, A. Nafady, J.H. Roudebush, S. Trupia, W.E. Geiger, One-electron oxidation of ruthenocene: reactions of the ruthenocenium ion in gentle electrolyte media, Inorg. Chem. 48 (2009) 2156–2165, https://doi.org/10.1021/ic802105b.
[56] V.N. Nemykin, G.T. Rohde, C.D. Barrett, R.G. Hadt, J.R. Sabin, G. Reina, et al., Long-range electronic communication in free-base meso-poly(ferrocenyl)-containing porphyrins, Inorg. Chem. 49 (2010) 7497–7509, https://doi.org/10.1021/ic101012a.
[57] A. Hildebrandt, D. Schaarschmidt, H. Lang, Electronically intercommunicating iron centers in di- and tetraferrocenyl pyrroles, Organometallics 30 (2011) 556–563, https://doi.org/10.1021/om100914m.
[58] D. Miesel, A. Hildebrandt, M. Korb, D. Schaarschmidt, H. Lang, Transition-metal carbonyl complexes of 2,5-Diferrocenyl-1-phenyl-1H-phosphole, Organometallics 34 (2015) 4293–4304, https://doi.org/10.1021/acs.organomet.5b00520.
[59] G. Gritzner, J. Kůta, Recommendations on reporting electrode potentials in nonaqueous solvents, Pure Appl. Chem. 56 (1984) 461–466, https://doi.org/10.1351/pac198456040461.
[60] A. Nafady, W.E. Geiger, Characterization of the successive one-electron oxidation products of the dicobalt fulvalenediyl (Fv) compound Co_2 Fv$(CO)_4$ and its phosphine-substituted product, Organometallics 27 (2008) 5624–5631, https://doi.org/10.1021/om800546d.
[61] I. Noviandri, K.N. Brown, D.S. Fleming, P.T. Gulyas, P.A. Lay, A.F. Masters, et al., The decamethylferrocenium/decamethylferrocene redox Couple: a superior redox standard to the ferrocenium/ferrocene redox couple for studying solvent effects on the thermodynamics of electron transfer, J. Phys. Chem. B 103 (1999) 6713–6722, https://doi.org/10.1021/jp991381+.
[62] J.R. Aranzaes, M.-C. Daniel, D. Astruc, Metallocenes as references for the determination of redox potentials by cyclic voltammetry - permethylated iron and cobalt sandwich complexes, inhibition by polyamine dendrimers, and the role of hydroxy-containing ferrocenes, Can. J. Chem. 84 (2006) 288–299, https://doi.org/10.1139/v05-262.
[63] M. Krejčik, M. Daněk, F. Hartl, Simple construction of an infrared optically transparent thin-layer electrochemical cell. Applications to the redox reactions of ferrocene, $Mn_2(CO)_{10}$ and $Mn(CO)_3$(3,5-di-t-butyl-catecholate)$^-$, J. Electroanal. Chem. 317 (1991) 179–187, https://doi.org/10.1016/0022-0728(91)85012-E.
[64] U.H.F. Bunz, 1,2_Diethynylferrocene, J. Organomet. Chem. 494 (1995) C8–C11, https://doi.org/10.1016/0022-328X(95)05509-N.
[65] M.I. Reyes Valderrama, R.A. Vázquez García, T. Klimova, E. Klimova, L. Ortiz-Frade, M. Martínez García, Synthesis of ferrocenyl-bearing dendrimers with a resorcinarene core, Inorganica Chim. Acta 361 (2008) 1597–1605, https://doi.org/10.1016/j.ica.2007.05.002.
[66] A. Akhoury, L. Bromberg, T.A. Hatton, Interplay of electron hopping and bounded diffusion during charge transport in redox polymer electrodes, J. Phys. Chem. B 117 (2013) 333–342, https://doi.org/10.1021/jp302157g.
[67] A.H. Schroeder, F.B. Kaufman, V. Patel, E.M. Engler, Comparative behavior of electrodes coated with thin films of structurally related electroactive polymers, J. Electroanal. Chem. 113 (1980) 193–208, https://doi.org/10.1016/S0022-0728(80)80021-0.
[68] D.A. Buttry, F.C. Anson, Electron hopping *vs.* molecular diffusion as charge transfer mechanisms in redox polymer films, J. Electroanal. Chem. 130 (1981) 333–338, https://doi.org/10.1016/S0022-0728(81)80402-0.
[69] K. Habermüller, M. Mosbach, W. Schuhmann, Electron-transfer mechanisms in amperometric biosensors, Fresenius. J. Anal. Chem. 366 (2000) 560–568, https://doi.org/10.1007/s002160051551.
[70] F. Mao, N. Mano, A. Heller, Long tethers binding redox centers to polymer backbones enhance electron transport in enzyme “wiring” hydrogels, J. Am. Chem. Soc. 125 (2003) 4951–4957, https://doi.org/10.1021/ja029510e.
[71] Y. Zhao, Y. Ding, J. Song, G. Li, G. Dong, J.B. Goodenough, et al., Sustainable electrical energy storage through the ferrocene/ferrocenium redox reaction in aprotic electrolyte, Angew. Chem. Int. Ed. 53 (2014) 11036–11040, https://doi.org/10.1002/anie.201406135.
[72] L. Cosimbescu, X. Wei, M. Vijayakumar, W. Xu, M.L. Helm, S.D. Burton, et al., Anion-tunable properties and electrochemical performance of functionalized ferrocene compounds, Sci. Rep. 5 (2015) 14117, https://doi.org/10.1038/srep14117.